JOURNAL OF MATERIALS SCIENCE **36** (2001) 623–629

Atomic force microscope studies of stainless steel: Surface morphology and colloidal particle adhesion

W. R. BOWEN*, R. W. LOVITT, C. J. WRIGHT
Centre for Complex Fluids Processing, Department of Chemical and Biological Process Engineering, University of Wales Swansea, Singleton Park, Swansea, SA2 8PP, UK
E-mail: r.bowen@swansea.ac.uk

An atomic force microscope has been used to image four commercial stainless steel samples of widely differing surface finishes. Analysis of the images allowed quantification of surface roughness over different area scales, 50×50 μm, 10×10 μm and 1×1 μm. The atomic force microscope was also used to measure directly the adhesion of a single polymer latex particle (radius $\sim$5 μm) to the surface in solution using the colloid probe technique. It was found that the adhesion increased with decreasing roughness, except for the smoothest surface which exhibited very regular surface features on the area scale most relevant to adhesion of the particle (1×1 μm). There was a good correlation between the variability of adhesion over each surface and the corresponding variability in surface roughness. Measurements of this type should prove useful in the technical/economic choice of surface finish for a particular purpose. As the colloid probe has dimensions comparable to those of bacteria and yeast cells, such measurements should especially be of value in the selection of surface finish likely to minimise bioadhesion. © *2001 Kluwer Academic Publishers*

1. Introduction

Adhesion of fine particles and colloids to surfaces has significance throughout the process and bioprocess industries. The types of equipment in which such adhesion may take place include pipelines, heat exchangers, fermentation vessels and membrane separators. Such adhesion can lead to loss of efficiency, contamination of products and loss of sterility. The balance of forces between a particle and a surface which results in adhesion has been the subject of much fundamental study. However, most such studies have focussed on flat, homogeneous surfaces and only recently have rough, heterogeneous surfaces received substantial attention [1]. Theoretical treatment of adhesion at such surfaces requires simplifying assumptions about the nature of the heterogeneity, generally resulting in only qualitative agreement with observed adhesion. Therefore, for practical purposes there remains a need for experimental methods which quantify the adhesion of particles to such surfaces.

Atomic force microscopy (AFM) [2] is a powerful imaging technique that, by scanning a sharp tip (typical end diameter 5–10 nm) over a surface, can produce topographical images which quantify surface morphology on an area scale comparable to that encountered by a colloid interacting with that surface. In addition, AFM can directly measure the force of adhesion of a single particle in a direction normal to the surface at which the interaction is taking place. This latter technique used involves the immobilisation of a single particle at the end of a tipless AFM cantilever, creating a "colloid probe" [3]. This measurement can be made in a process relevant environment, air or liquid. Thus, AFM is uniquely able to investigate both surface roughness and its influence on small particle adhesion. The colloid probe technique has been mostly used to quantify the forces acting during the approach of particles to surfaces [3–5], for example, electrical double layer interactions. There have also been studies of adhesion of hard inorganic particles to surfaces [6–9] and of deformable particles to surfaces [10–13]. The influence of particle surface roughness has been studied by measuring the adhesion of colloid probes made of different materials to atomically flat surfaces in a nitrogen atmosphere [14]. However, the planar surfaces at which adhesion has been measured have mostly been relatively smooth. Theoretically, when the topography has peaks and troughs that are of similar dimensions to the particle the adhesion is increased or decreased relative to that measured at a flat surface depending on where the interaction occurs [1]. When the roughness dimensions are much smaller than the particle size the adhesion is expected to be substantially reduced.

Stainless steel is one of the materials most commonly used in process plant fabrication. The quality of the metal surface finish required is an important economic

* Author to whom all correspondence should be addressed.

consideration that needs to be balanced with the influence the surface roughness has on process efficiency. There are some published studies of the use of AFM to study the influence of metal surface finishing on topography [15], but none also report the influence of roughness on adhesion. The present paper describes an AFM study of the surface properties of four stainless steel surfaces—two steel plate surfaces used in the chemical, pharmaceutical, dairy and nuclear industries, and two steel sheet surfaces used for aesthetic finishes of microwaves, fridges and food work surfaces [16]. The adhesion of a polymer latex colloid probe to these four surfaces in liquid has also been quantified. Such deformable latex spheres may be considered to be model systems. Their dimensions and non-specific surface interactions will be comparable to those of bacteria and yeast cells [17], but they may be studied in the atomic force microscope without the need for maintaining cell viability.

2. Materials and methods

Stainless steel (304) samples were obtained from Sillavan Metal Services (Wolverhampton UK). The two plate surfaces were termed Super Smooth (BS1449 No 8 Type) and Coarse Ground Grit (BS1449 No 3A). The two sheet surfaces were termed Super Bright (BS1449 No 7) and Long Grain Brush (BS1449 No 5). Table I lists the manufacturer's roughness specifications. It may be seen that they cover a wide range of mean roughness (R_a) and reflectivity. Prior to imaging surfaces were washed in ethanol, rinsed with deionised water, sonicated for 30 minutes, rinsed again with deionised water and finally left to dry. After imaging the surfaces were then soaked in 0.5 M NaOH, rinsed with deionised water and placed in the AFM liquid cell ready for adhesion measurements. Soaking in NaOH was performed so that the experimental metal surface would have undergone a cleaning procedure comparable to that used for bioreactors. Force measurements were made in 10^{-2} M NaCl pH 7.0. All experiments were performed at 25° C.

The Atomic Force Microscope used for imaging was an Autoprobe (CP-100) (Themomicroscopes). Surfaces were imaged in contact mode in air using silicon cantilevers with a high aspect ratio and typical tip diameter of 10 nm (Ultralevers, Themomicroscopes). The scan rate of imaging was 1 Hz with a constant force of $\sim 10^{-8}$ N. Relative humidity was constant at 33%. For adhesion measurements an Explorer (Themomicroscopes) instrument was used.

TABLE I Surface roughness measurements for four stainless steel samples

	Manufacturer's Specifications		AFM R_a measurements (nm)			
Surface Finish	R_a (nm)	Reflectivity	50 × 50 μm image	10 × 10 μm image	1 × 1 μm image	Mean of 50 1 × 1 μm areas***
Super Bright	50	58/63	7.9	4.3	1.90	1.92 (±0.65)
Super Smooth	200/400*	28/34*	43.4	9.5	0.37	2.80 (±1.63)
Long Grain Brush	200	30/40*	111.9	22.0	3.13	4.00 (±2.27)
Coarse Ground Grit**	2500	∼10	130.7	32.2	2.42	5.39 (±2.97)

*Allowable range **80 Grit. ***Standard deviations in brackets.

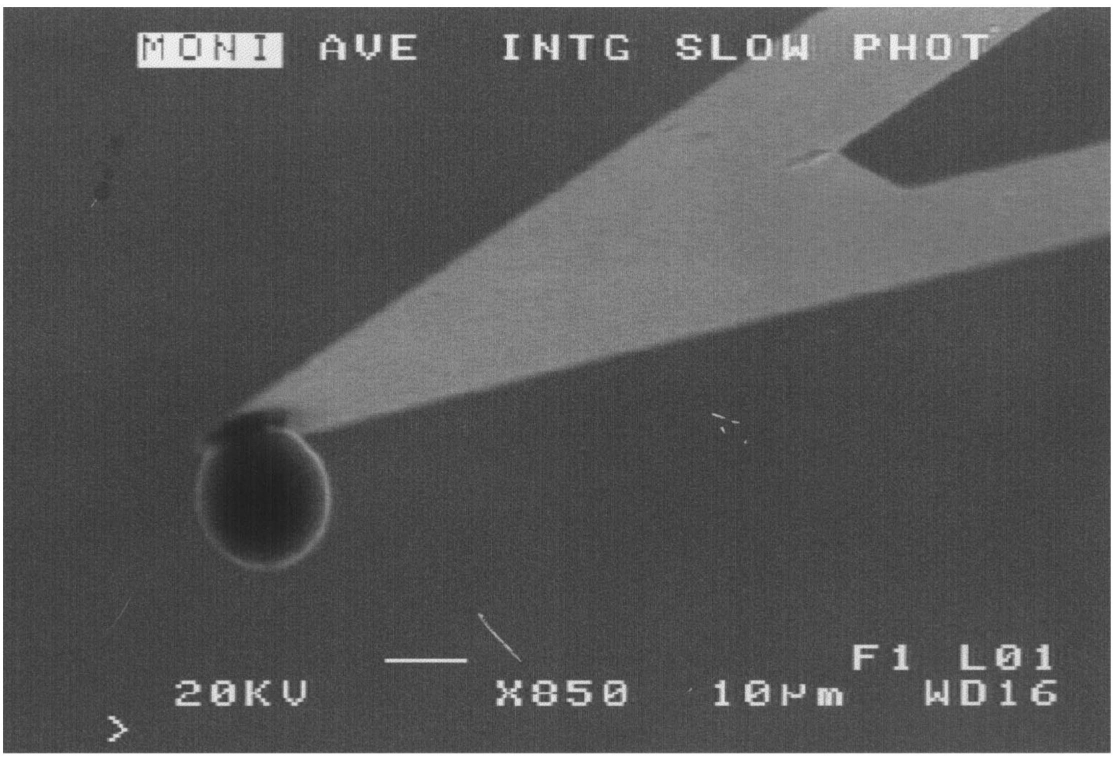

Figure 1 SEM image of a polystyrene latex colloid probe.

Colloid probes were constructed by attaching a polystyrene sphere (Sigma, catalogue number LB-120, radius ∼5 μm) with epoxy resin (DP 105, Scotch-Weld) to a standard V-shaped AFM tipless cantilever (Themomicroscopes). The polystyrene spheres were stored in solution and for immobilisation a droplet was placed on a glass slide adjacent to a droplet of glue. The glass slide was then placed in a micromanipulator (Singer Instruments) which allowed fine control of the cantilever position. The tipless cantilever was coated with a small quantity of glue at its apex and manipulated so as to pick up a sphere from the slide. The use of the micromanipulator allowed the sphere to be precisely located at the apex of the V-shaped cantilever with the minimum amount of glue, ensuring that neither the lower surface of the sphere nor the reflective gold coating of the back of the cantilever was contaminated by glue. Such a colloid probe is shown in Fig. 1.

AFM allows measurement of the force between the colloid probe and metal surface as a function of separation, where the separation is varied using a piezo crystal. A laser beam reflected from the back of the cantilever falls onto a position-sensitive photodiode that detects small changes in the cantilever deflection. To

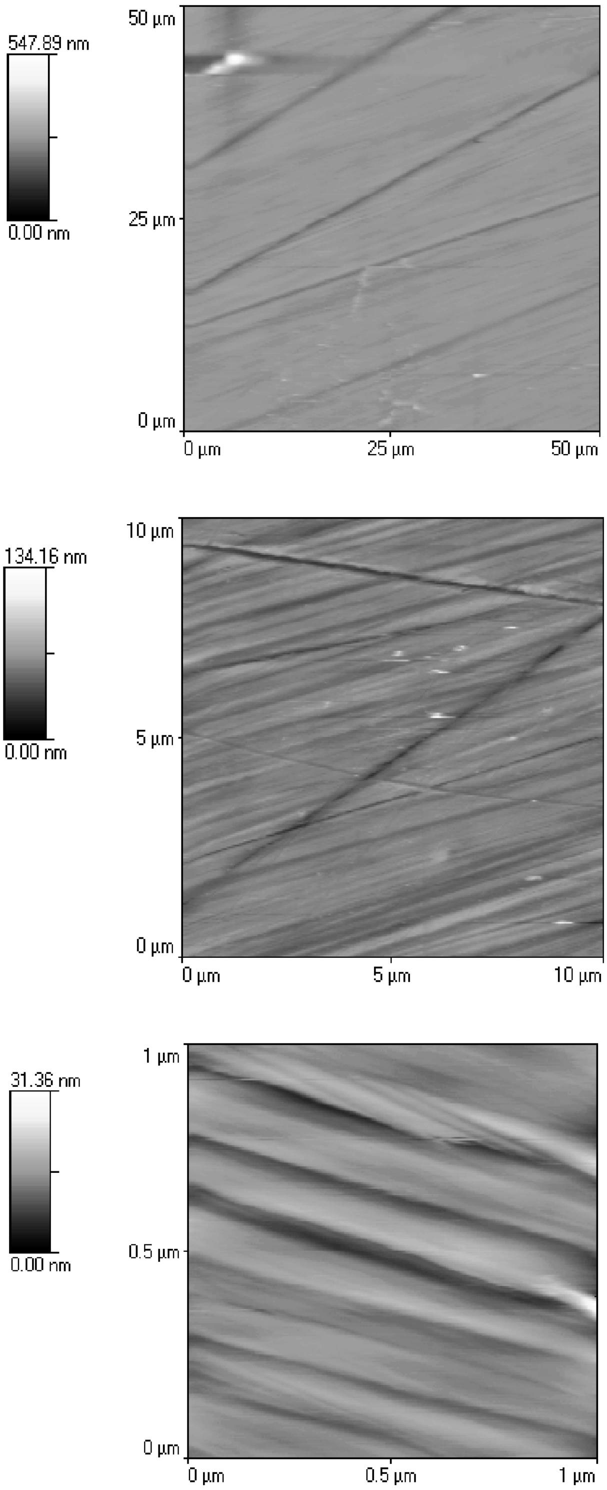

Figure 2 AFM contact mode images in air of a Super Bright surface finish stainless steel: 50 × 50 μm, 10 × 10 μm and 1x1 μm areas.

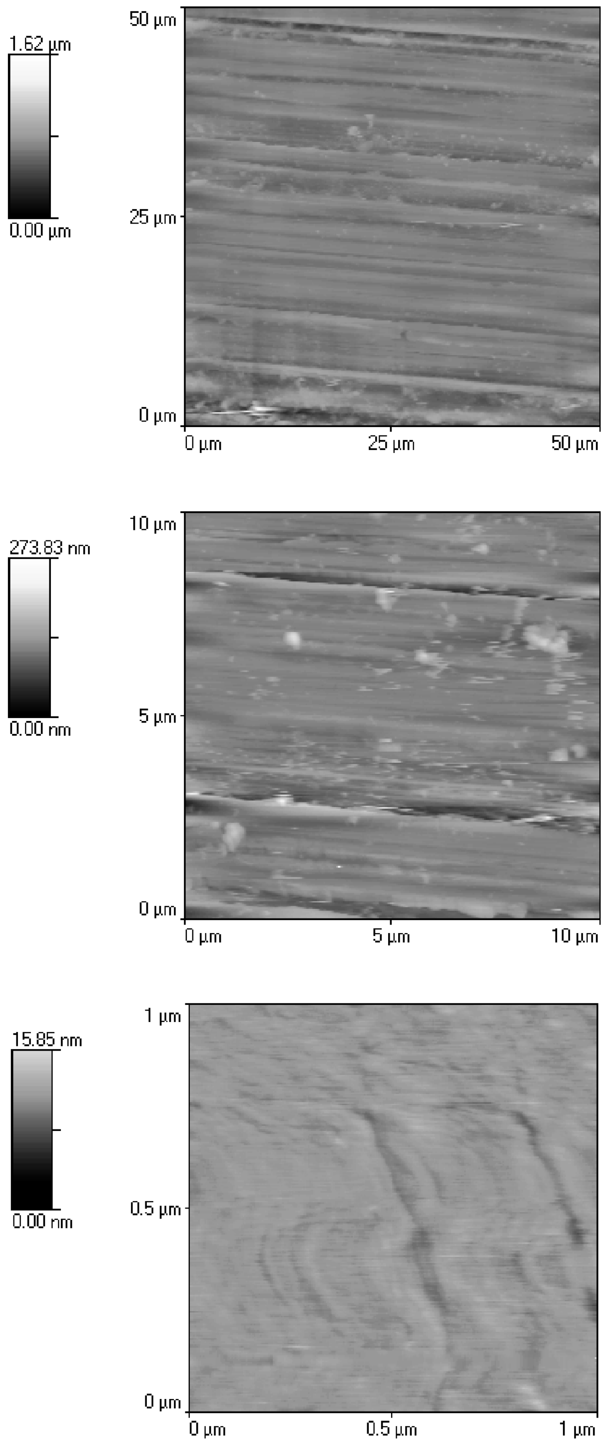

Figure 3 AFM contact mode images in air of a Super Smooth surface finish stainless steel: 50 × 50 μm, 10 × 10 μm and 1 × 1 μm areas.

convert the deflection to a force it is necessary to know the spring constant of the cantilever and to define the zero of force. The cantilever spring constant can vary substantially from that specified by the manufacturer, thus each cantilever used was calibrated directly by the method of Cleveland *et al*. [18]. This well established method is based on measurement of the variation of resonance frequency on addition to the apex of the cantilever of small tungsten spheres of known mass. The zero of force was chosen where the deflection was independent of the piezo position (where the colloid probe and the metal surface were far apart). The probe movement was kept constant in all experiments at 0.1 μm/s.

3. Results and discussion

3.1. Surface characteristics—image analysis

The four surfaces were imaged over areas of $50 \times 50\ \mu$m, $10 \times 10\ \mu$m and $1 \times 1\ \mu$m, Figs 2–5. In these Figures, the colour intensity shows the vertical profile of the surfaces, with light regions being the highest points and dark regions being the lowest points. At the $50 \times 50\ \mu$m and $10 \times 10\ \mu$m level, all of the surfaces have scratches in the polishing direction, though these are somewhat less-defined for the Coarse Ground Grit at $10 \times 10\ \mu$m. These scratches remain well-defined at the $1 \times 1\ \mu$m level for the Super Bright finish. For the

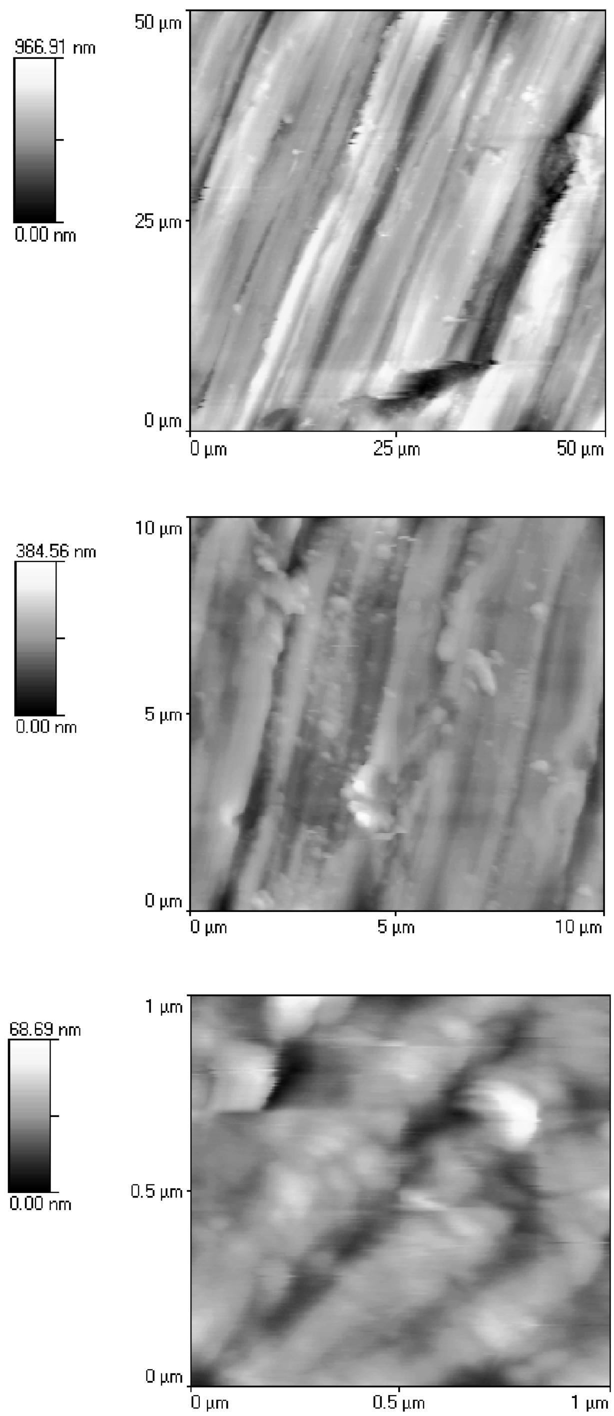

Figure 4 AFM contact mode images in air of a Long Grain Brush surface finish stainless steel: $50 \times 50\ \mu$m, $10 \times 10\ \mu$m and $1 \times 1\ \mu$m areas.

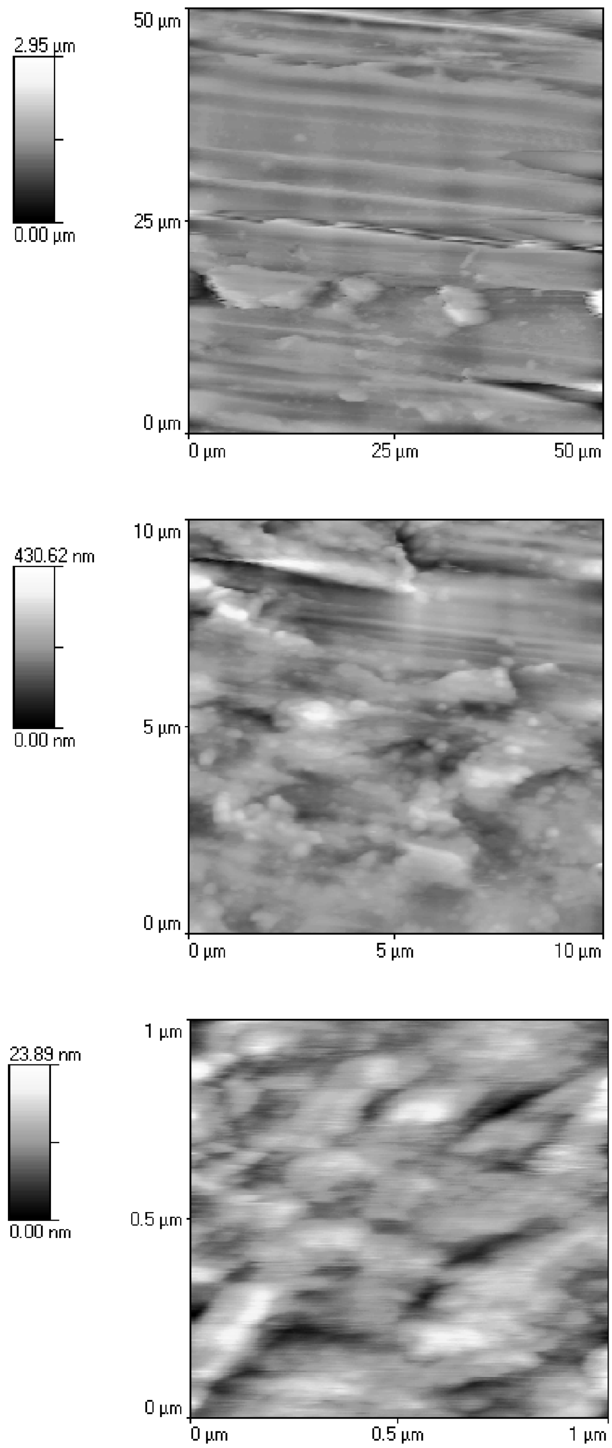

Figure 5 AFM contact mode images in air of a Coarse Ground Grit surface finish stainless steel: $50 \times 50\ \mu$m, $10 \times 10\ \mu$m and $1 \times 1\ \mu$m areas.

other surfaces the scratches are less-defined and have rough edges leading to an overall granular appearance at this level.

Mean surface roughness [19] (R_a) may be calculated from the digitally stored data of Figs 2–5. This is defined as the arithmetic mean of the deviations in height from the image area mean value ($\bar{Z}$),

$$R_a = \frac{1}{n}\sum_{i=1}^{n} \left| Z_i - \bar{Z} \right| \qquad (1)$$

where Z_i is the height of each datum. Values are reported in Table I. It may be seen that the values at $50 \times 50\,\mu$m and $10 \times 10\,\mu$m are in the same sequence as that for the manufacturer's specification (taking both roughness and reflectivity into account), but the magnitudes of the values vary with the image area used as Equation 1 does not have a term accounting for the area analysed. (The manufacturer's values were obtained using a Surtronic (Taylor Hobson) surface roughness measurement instrument with a 5 μm radius stylus tip, expressed as the average for five 0.8 mm lines.) For the single images the average roughness values at $1 \times 1\,\mu$m do not follow the same sequence as such a small area is not sufficiently representative of the sample. Hence, the Table also shows mean roughness values for 50 $1 \times 1\,\mu$m areas selected systematically from a grid on the $10 \times 10\,\mu$m images. These mean roughness values now follow the sequence specified by the manufacturer.

It should also be noted that the ratio of the standard deviation of these mean values to the mean values themselves (normalised standard deviation) is significantly smaller for the Super Bright surface (ratio 0.34) compared to the other surfaces (ratios in range 0.55–0.58) showing a lesser variation in roughness in the former case. The area of contact of a deformable sphere of colloidal dimensions depends on the radius of the sphere and the applied force [20, 21], but may approach 1 μm^2 for a sphere of the dimensions used in the present work.

3.2. Colloidal particle adhesion

To measure the adhesion force, the colloid probe was first brought into momentary contact with the stainless steel surface with a specified normalised loading force, 40 mN/m for all measurements (normalised force = force/probe radius). (The loading force may have some influence on the magnitude of the pull-off (adhesion) force [7], so it may be important to keep it constant for comparative measurements.) The colloid probe was then retracted from the surface.

Fig. 6 shows four representative normalised force-distance retraction curves measured at different locations on the Super Bright surface in 10^{-2} M NaCl at pH 7.0. They illustrate the variation of shape of the adhesion components of the force-distance curves that were measured within an area of $50 \times 50\,\mu$m. From *A* to *B* the probe and metal surface were in contact and moving together. They remained in contact from *B* to

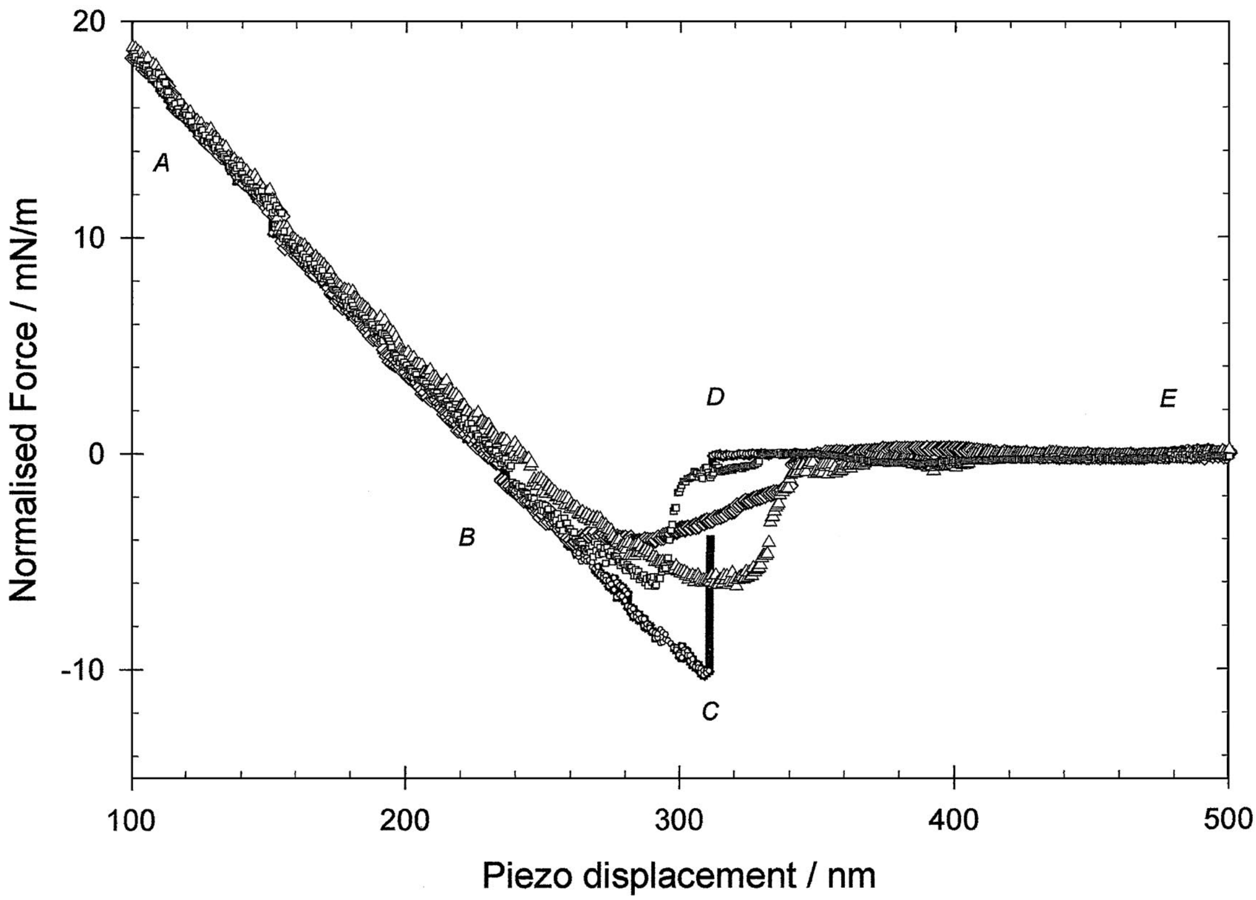

Figure 6 Four representative normalised force-distance retraction curves measured for a colloid probe at different locations on a Super Bright surface finish stainless steel. 10^{-2} M NaCl, pH 7.0.

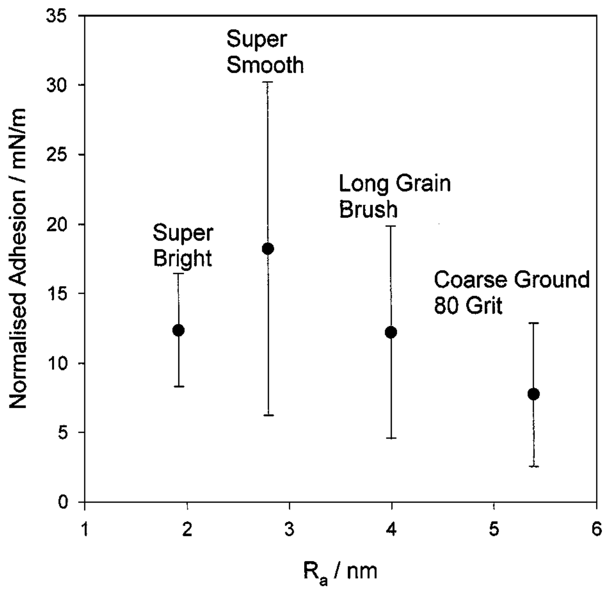

Figure 7 Normalised adhesion forces (adhesion force/colloid probe radius) for a polystyrene latex colloid probe at four stainless steel surfaces versus mean roughness over an area of 1×1 μm. Adhesion forces are the mean of 50 measurements on each surface. The error bars are a standard deviation in length in each direction.

C, though the curvature of some of the data lines shows that over this interval they had some movement relative to each other. Contact between the probe and surface was finally broken in the region *C* to *D*. The difference in force between *C* and *D* is a quantitative measure of the adhesion force. In some cases adhesion was broken very sharply at *C*. In others there was staggered breaking of surface contact. This shows the heterogeneity of adhesion over the metal surface. From *D* to *E* the probe and metal surface moved independently, the probe was no longer in contact with the surface.

For each of the four steel surfaces, 50 force-distance curves were measured systematically over an area of 50×50 μm. The resulting mean adhesion values are shown in Fig. 7, plotted against the mean roughness values over areas of 1×1 μm (Table I). The error bars are a standard deviation in length in each direction. The overall pattern is for increasing adhesion as the roughness decreases in the sequence Coarse Ground Grit, Long Grain Brush and Super Smooth. However, the adhesion then decreases for the smoothest surface, Super Bright. The values of the normalised standard deviations for adhesion are 0.33 for Super Bright and in the range 0.60–0.65 for the other surfaces. These values follow closely those for the mean roughness (Section 3.1), showing how closely adhesion and roughness are related. The AFM images of the surfaces, Figs 2–5, show that the characteristic size of the roughness features over an area of 1×1 μm is significantly smaller than the size of the probe. Therefore, the main expected effect [1] of the roughness is to reduce the area of contact between probe and surface and so reduce adhesion, explaining the sequence for Coarse Ground Grit, Long Grain Brush and Super Smooth. In this sense, the lower adhesion for the Super Bright surface is anomalous, possibly associated with the greater regularity of the surface features at the 1×1 μm length scale.

4. Conclusions

The present paper has shown AFM images of four commercial stainless steel samples of widely differing surface finishes. Analysis of the images allowed quantification of surface roughness over different area scales, 50×50 μm, 10×10 μm and 1×1 μm. It was found that the sequence of mean roughness values agreed with the manufacturer's specification, which was measured over a much greater range using a probe of characteristic dimensions almost three orders of magnitude greater than the AFM tip.

The atomic force microscope was also used to measure directly the adhesion of a single polymer latex particle to the surface in solution. It was found that the adhesion increased with decreasing roughness, except for the smoothest surface which exhibited very regular surface features on the area scale most relevant to adhesion of the particle (1×1 μm). There was a good correlation between the variability of adhesion over each surface and the corresponding variability in surface roughness. The results show that of the two plate steels used for equipment manufacture (Coarse Ground Grit and Super Smooth), adhesion is less at the rougher surface. For the two sheet steels used for aesthetic finishes (Long Grain Brush and Super Bright) adhesion is very comparable despite the differences in surface roughness. Measurements of this type should prove useful in the technical/economic choice of surface finish for a particular purpose. As the colloid probe has dimensions comparable to those of bacteria and yeast cells, such measurements should especially be of value in the selection of surface finish likely to minimise bioadhesion.

Acknowledgement

This work was funded by the UK Biotechnology and Biological Sciences Research Council.

References

1. J. Y. WALZ, *Adv. Colloid Interface Sci.* **74** (1998) 119.
2. G. BINNIG, C. F. QUATE and CH. GERBER, *Phys. Rev. Lett* **56** (1996) 930.
3. W. A. DUCKER, T. J. SENDEN and R. M. PASHLEY, *Langmuir* **8** (1992) 1831.
4. D. T. ATKINS and R. M. PASHLEY, *Ibid.* **9** (1993) 2232.
5. H-J. BUTT, M. JASCHKE and W. DUCKER, *Bioelectrochemistry Bioenergetics* **38** (1995) 191.
6. S. VEERAMASUNEI, M. R. YALAMANCHILI and J. D. MILLER, *J. Colloid Interface Sci.* **184** (1996) 594.
7. G. TOIKKA, R. A. HAYES and J. RALSTON, *Ibid.* **180** (1996) 329.
8. M. PIERCE, J. STUART, A. PUNGOR, P. DRYDEN and V. HLADY, *Langmuir* **10** (1994) 3217.
9. W. R. BOWEN, N. HILAL, R. W. LOVITT and C. J. WRIGHT, *Colloids and Surfaces A: Physicochem. Eng. Aspects* **157** (1999) 117.
10. S. BIGGS and G. SPINKS, *J. Adhesion Sci. Technol.* **12** (1998) 461.
11. W. R. BOWEN, N. HILAL, R. W. LOVITT and C. J. WRIGHT, *Colloids and Surfaces A: Physicochem. Eng. Aspects* **136** (1998) 231.
12. *Idem., J. Membrane Sci.* **139** (1998) 269.
13. *Idem., ibid.* **154** (1999) 205.
14. D. M. SCHAEFER, M. CARPENTER, B. GADY, R. REIFENBERGER, L. P. DEMEJO and D. S. RIMAI. *J. Adhesion Sci. Technol.* **9** (1995) 1049.

15. J. R. SMITH, S. A. CAMPBELL and F. C. WALSH, *Trans. IMF* **76** (1998) B53.
16. Personal Communication Sillavan Metal Services Ltd Wolverhampton UK.
17. P. F. LUCKHAM and P. G. HARTLEY, *Adv. Colloid and Interface Sci* **49** (1994) 341.
18. J. P. CLEVELAND, S. MANNE, D. BOCEK and P. K. HANSMA, *Rev. Sci. Instrum.* **64** (1993) 403.
19. BS 1134: Part 1, British Standards Institution, 1988.
20. B. V. DERJAGUIN, V. M. MULLER and Y. P. TOPOROV, *J. Colloid and Interface Sci.* **53** (1975) 314.
21. V. MULLER, V. S. YUSHENKO and B. V. DERJAGUIN, *ibid.* **77** (1980) 91.

Received 1 December 1999
and accepted 17 May 2000